Journal of Molecular Spectroscopy **203,** 330–338 (2000)
doi:10.1006/jmsp.2000.8187, available online at http://www.idealibrary.com on IDEAL®

Fourier Transform Spectroscopy of the $A'^1\Pi$–$X^1\Sigma^+$ System of CaO

C. Focsa,* A. Poclet,* B. Pinchemel,* R. J. Le Roy,† and P. F. Bernath†

*Laboratoire de Physique des Lasers, Atomes et Molécules, UMR CNRS 8523, Centre d'Etudes et de Recherches Lasers et Applications, Université des Sciences et Technologies de Lille, 59 655 Villeneuve d'Ascq Cedex, France; and †Department of Chemistry, University of Waterloo, Waterloo, Ontario, Canada N2L 3G1

Received May 24, 2000

The $A'^1\Pi$–$X^1\Sigma^+$ near-infrared system of CaO was observed for the first time at high resolution using a Fourier transform spectrometer. The $A'^1\Pi$–$X^1\Sigma^+$ chemiluminescence was excited in a Ca + N_2O flame produced in a Broida-type oven. More than 3000 rotational lines, classified into 19 bands involving the $A'^1\Pi$ $0 \le v' \le 3$ and the $X^1\Sigma^+$ $1 \le v'' \le 7$ vibrational levels were measured in the 4000–10 000 cm^{-1} region with a precision of 0.005 cm^{-1}. The $X^1\Sigma^+$ ($v = 0$, 1) millimeter-wave and $X^1\Sigma^+$ ($v =$ 0–3) infrared data available in the literature were merged with our new electronic data in order to obtain improved Dunham constants for the ground state of CaO. Very peculiar perturbations are observed in the higher vibrational levels of the $A'^1\Pi$ state, so the upper levels of transitions with $v' = 2$ and 3 were represented by term values in our least-squares analysis. The interaction of the $A'^1\Pi$ ($v \ge 2$) levels with the nearby $b^3\Sigma^+$ (v–2) levels has been detected. An extended set of $A'^1\Pi$ ($v = 0$–3) data has been obtained which is suitable for use in a future multistate deperturbation analysis of the $a^3\Pi \sim A'^1\Pi \sim b^3\Sigma^+ \sim A^1\Sigma^+$ complex of excited states. The new near-infrared spectra of the $A'^1\Pi$–$X^1\Sigma^+$ transition of CaO also permits the first direct high-resolution linkage between the orange and green systems and the near-infrared bands. © 2000 Academic Press

I. INTRODUCTION

The first spectroscopic studies of the calcium oxide were conducted by Mahanti (*1*), Brodersen (*2, 3*), and Meggers (*4*) in the early 1930s. They remarked on the very complex appearance of the spectrum, with numerous bands extending from the ultraviolet to the near-infrared, and tried various schemes for arranging these bands into systems and giving vibrational assignments. In 1945, Lejeune (*5*) tried to clarify the structure of the orange and green bands, Lejeune and Rosen (*6*) contributed bandhead equations for the blue and UV bands, and Lejeune and Rosen (*6*) collected all of the known systems into a term scheme.

In the early 1950s, Hultin and Lagerqvist (*7*) photographed the 7000–11 000 Å spectral region and provided a crucial analysis of a $^1\Sigma$–$^1\Sigma$ infrared system, which was subsequently named the *A*–*X* system. They remarked on the presence of numerous perturbations in the upper state and described them in great detail. Hultin and Lagerqvist's study of the $A^1\Sigma^+$–$X^1\Sigma^+$ system of CaO remains the reference study of this transition. Lagerqvist (*8*) also gave a rotational analysis of an ultraviolet ($C^1\Sigma^+$–$X^1\Sigma^+$) system and a blue ($B^1\Pi$–$X^1\Sigma^+$) system of CaO. In this study, the common lower state of the three systems (IR, blue, and UV) was called the ground state, although no direct evidence was presented for that assignment. The study of the infrared system (*7*) gave access to the $v = 0$ to 3 vibrational levels of the ground state, and the $X^1\Sigma^+$ ($v =$ 4) level was reached in one band of the UV system (*8*).

Supplementary data for this article are available on IDEAL (http://www.idealibrary.com) and as part of the Ohio State University Molecular Spectroscopy Archives (http://msa.lib.ohio-state.edu/jmsa_hp.htm).

In 1968, Brewer and Hauge (*9*) recorded the $\Delta v = -1$, -2, and -3 sequences of the *A*–*X* system with a 1.5-m spectrograph and performed bandhead measurements giving vibrational assignments involving $v' \le 12$ and $v'' \le 14$ levels. Four bands (namely, 3–5, 4–6, 5–7, and 6–8) were also recorded with a 6.1-m spectrograph, allowing rotational analysis and the determination of molecular constants for $v'' \le 8$ vibrational levels of the ground state.

The data of Refs. (*7*) and (*9*) were used by Field in 1974 for a deperturbation analysis (*10*) leading to the assignment of the $a^3\Pi$ and $A'^1\Pi$ states of CaO (and also for BaO and SrO) as the perturber states observed by Hultin and Lagerqvist (*7*) in their study of the *A*–*X* system. The analysis of Field undoubtedly proved the $^1\Sigma^+$ symmetry of the ground state of CaO (also that of BaO and SrO), correcting an erroneous result obtained by Brewer and Wang (*11*) from an Ar-matrix study. At about the same time, Field *et al.* (*12*) reported the observation of the $A'^1\Pi$–$X^1\Sigma^+$ system at low resolution. Twenty bandheads were identified, involving high-vibrational levels of the $A'^1\Pi$ state ($9 \le v' \le 21$), but only the $v = 0$, 1, and 2 vibrational levels of the $X^1\Sigma^+$ ground state. In the early studies, CaO was produced in arc discharges, but in the mid-1970s Broida-type ovens started to become the standard source, using the Ca + N_2O or Ca + O_3 reactions (*12, 13*).

The availability of cw single-mode lasers offered the opportunity for high-resolution studies of the very complex structure of the orange and green bands of CaO. By using various laser-induced fluorescence and double-resonance techniques, Field's group at MIT performed an enormous quantity of work on these bands (*14–20*) and provided an interpretation for the

0022-2852/00 $35.00

electronic structure of CaO. The $A'^1\Pi$ and $a^3\Pi$ states were the lower states for all the systems observed: $D,d^{1,3}\Delta$–$a^3\Pi$ (*14, 15*), $c^3\Sigma^+$–$a^3\Pi$ (*16*), $C'^1\Sigma^+$–$A'^1\Pi$ (*17*), $e^3\Sigma^-$–$a^3\Pi$ and $E^1\Sigma^-$–$A'^1\Pi$ (*18*), $F^1\Pi$–$A'^1\Pi$ and $B^1\Pi$–$A'^1\Pi$ (*19*), with the sole exception of the $B^1\Pi$–$b^3\Sigma^+$ (1, 1) band (*20*).

Highly precise millimeter-wave measurements of CaO were also performed with eight pure rotational lines recorded in the $v = 0$ and 1 vibrational levels of the $X^1\Sigma^+$ ground state (*21, 22*). The vibrational spectrum was investigated by infrared laser absorption spectroscopy (*23, 24*), giving access to $X^1\Sigma^+$ ($v \leq 3$). The millimeter-wave and infrared data were used by Blom *et al.* (*25*) to derive Dunham constants for the $X^1\Sigma^+$ ground state of CaO (in parallel with their study of SrO and BaO). Due to the intrinsic precision of these measurements, the constants so derived were the most accurate to date. Calcium oxide was also a target for several theoretical studies, focusing on the nature of the ground state (*26*), or more generally, on the electronic structure of the molecule (*27–29*).

As part of a measurement campaign on the alkaline–earth oxides (CaO, SrO, and BaO), we have recorded the near-infrared spectrum of CaO using a Fourier transform spectrometer (FTS). The $A'^1\Pi$–$X^1\Sigma^+$ system is observed for the first time at high resolution in the 4000–10 000 cm^{-1} spectral range. The $A^1\Sigma^+$–$X^1\Sigma^+$ system was also observed in the 10 000–16 000 cm^{-1} region, but its analysis will be reported elsewhere (*30*). The rotational analysis of the $A'^1\Pi$–$X^1\Sigma^+$ transition presented here involves vibrational levels of the lower state up to $v'' = 7$ and allows us to improve the Dunham constants of the $X^1\Sigma^+$ ground state of CaO. Our new data are fitted together with millimeter-wave (for $v'' = 0$ and 1 (*21, 22*)) and infrared (for the $v'' = 0$–3 (*23, 24*)) data from the literature to obtain improved Dunham constants. The $A'^1\Pi$ upper state is affected by significant perturbations and has been consequently represented by term values for $v' = 2$ and 3 in our least-squares treatment and band constants for $v' = 0$ and 1. Some new aspects of the interactions taking place in the $a^3\Pi \sim A'^1\Pi \sim b^3\Sigma^+ \sim A^1\Sigma^+$ manifold of excited states have been noticed.

II. EXPERIMENTAL DETAILS

The CaO molecule was produced in a Broida-type oven (*31, 32*) by the exothermic reaction between Ca and N_2O (*13*). The Ca vapor was obtained by heating a few grams of Ca metal in an alumina crucible in a tungsten wire basket (~40 A current). A flow of Ar carrier gas (typical pressure ~5 Torr) entrained the Ca vapor, which was then mixed with N_2O gas. The optimum flame intensity and stability were obtained by separately adjusting the Ar and N_2O partial pressures. Under these conditions, a stable CaO chemiluminescence was obtained for several hours.

A Bruker IFS 120 HR Fourier transform spectrometer, modified to record double-sided interferograms, was used to record the near-infrared emission spectrum of CaO. The chemiluminescence was focused on the entrance aperture of the FTS by two CaF_2 lenses. Using a spherical mirror on the "back" side of the flame resulted in a gain of as much as 30% in the signal.

An InSb detector was used to cover the 1800–10 000 cm^{-1} spectral region (we also recorded the CaO emission in the 10 000–16 000 cm^{-1} range by using a Si photodiode (*30*)). The 1800–10 000 cm^{-1} region was split into two parts: 1800–6600 cm^{-1} and 5300–10 000 cm^{-1}, by using red- and/or blue-pass filters. The instrumental resolution was set at 0.03 cm^{-1} (higher resolution was not necessary, as the linewidth of the CaO lines was about 0.04 cm^{-1}). A total of 100 scans were co-added for each spectrum to obtain a good signal-to-noise ratio.

The line positions were measured by fitting Voigt lineshape functions to the experimental lines in a nonlinear, least-squares procedure included in the WSpectra program written by Dr. M. Carleer at the Laboratoire de Chimie Physique Moléculaire of the Université Libre de Bruxelles. The precision of our measurements is estimated to be ± 0.005 cm^{-1} for medium-strength, unblended lines. The air-to-vacuum conversion of the wavenumbers was carried out using Edlén's formula (*33, 34*). The absolute calibration of the wavenumber scale was achieved using the positions of Ca I atomic lines measured by Engleman (*35*). Four strong atomic lines were present on the 1800–6600 cm^{-1} spectrum, and we used them to calibrate this spectral range. The 5300–10 000 cm^{-1} region was then calibrated using about 30 intense, isolated CaO molecular lines, common to the two spectra (in the overlapping 5300–6600 cm^{-1} region). The absolute accuracy of the wavenumber scale is estimated to be ± 0.005 cm^{-1}. In some of our experiments, an Ar pen lamp was lit for several minutes, and this explains the presence of Ar atomic lines in our spectra. However, we preferred to use the Ca I lines for calibration, as they share the same optical path as the CaO chemiluminescence.

III. RESULTS

1. Observations and Assignments

An overview spectrum of the $A'^1\Pi$–$X^1\Sigma^+$ transition observed between 4000 and 10 000 cm^{-1} is displayed in Fig. 1. A vibrational assignment (indicating the position of the bandheads) of the identified bands is also given in this figure. A total of 19 bands were identified, involving the $0 \leq v' \leq 3$ vibrational levels of the $A'^1\Pi$ upper state and $1 \leq v'' \leq 7$ vibrational levels of the $X^1\Sigma^+$ ground state. A list of these bands (including band origins and, when observed, bandheads) is given in Table 1 in the form of a Deslandres table.

The rotational assignment of the lines was (until a certain stage of the work) quite straightforward, as the bands present a "classical" P–Q–R structure (shaded to lower wavenumbers), typical for a $^1\Pi$–$^1\Sigma$ transition. An example of such a band can be seen in Fig. 2, where an expanded portion of the 0–5 band is displayed. The rotational assignment was particularly easy for the $v' = 0$ bands, as the $A'^1\Pi$ ($v' = 0$) level is not visibly perturbed (at least up to the maximum J value of 80 that we

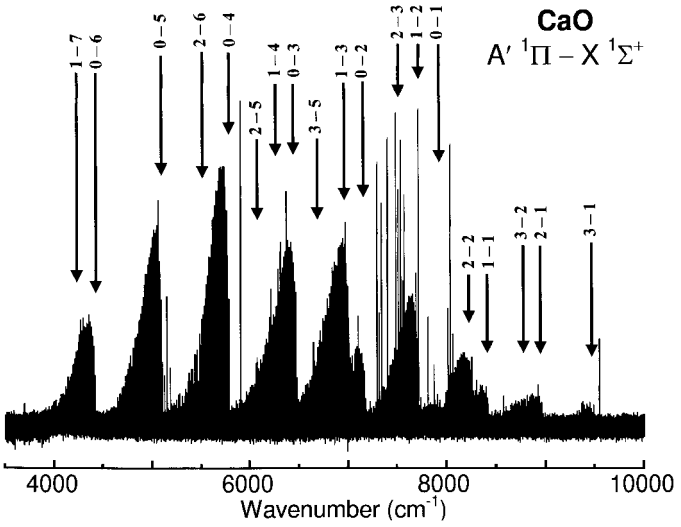

FIG. 1. An overview of the $A'^1\Pi$–$X^1\Sigma^+$ chemiluminescence spectrum of CaO recorded by Fourier transform spectroscopy. The vibrational assignment of the 19 bands identified is indicated.

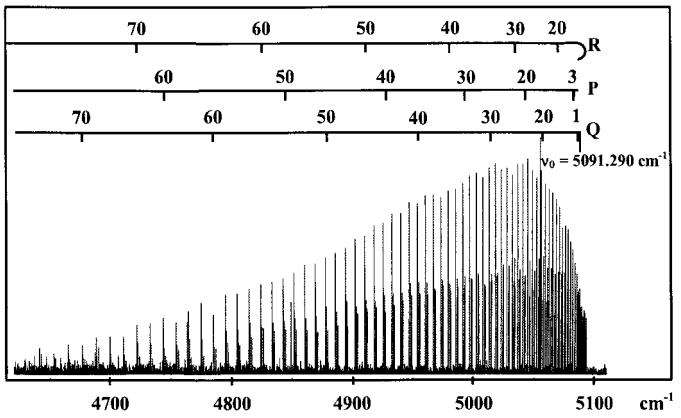

FIG. 2. An expanded portion of the $A'^1\Pi$–$X^1\Sigma^+$ emission spectrum of CaO displaying the 0–5 band. The rotational assignments are indicated.

observed), and especially in the long-wave part of the spectrum (~4000 to 7000 cm^{-1}), where the 0–v'' bands are the strongest (see Fig. 1). For these bands a Loomis–Wood program was used successfully to get quick results.

The assignments of these bands gave us improved constants for the $v'' = 2$–6 vibrational levels of the $X^1\Sigma^+$ ground state that were used in the subsequent assignment of bands originating from the $v' = 1$, 2, and 3 vibrational levels of the $A'^1\Pi$ state. Very accurate constants derived from the millimeter-wave and infrared studies of CaO (*21–25*) for the $v'' = 0$–3 vibrational levels of the ground state are already available, and we also used them in making our assignments.

Accurate ground state constants were crucial, because the $A'^1\Pi$ upper state is heavily perturbed in the $v' = 2$ and 3 vibrational levels. In this case, ground state combination differences were used in order to make the assignments. However, no extra lines were observed (in contrast with our measurements of the $A^1\Sigma^+$–$X^1\Sigma^+$ systems of BaO (*36*), SrO (*37*), and CaO (*30*)). This implies that the observed vibrational levels of the $A'^1\Pi$ state are rather "continuously" perturbed by the vibrational levels of other electronic state(s) which are present in their vicinity. The crossing of levels, which would generate extra lines, does not occur for the observed J range.

When using our Loomis–Wood program, perturbations appear as increasing deviations from the expected line positions. We manually double-checked and assigned all the lines of the bands involving the highly perturbed $A'^1\Pi$ $v' = 2$ and 3 vibrational levels. Once a set of term values was derived for a specific $A'^1\Pi$ v' vibrational level, they were then used to assign the other v'–v'' bands that share the same upper level.

We noted that there was very good agreement (systematic discrepancies < 0.01 cm^{-1}) between the combination differences for our $A'^1\Pi$ term values and those computed for the $v' = 0$, 1, and 2 vibrational levels from the experimental lines

TABLE 1
Deslandres Table of the 19 $A'^1\Pi$–$X^1\Sigma^+$ Vibrational Bands Assigned

v′ \ v″	0	1	2	3	4	5	6	7
0	–	**7885.700** *7174.476*	**7172.877** *6471.237*	**6469.598** *5777.433*	**5775.761** *5093.017*	**5091.290** *4417.866*	**4416.059**	–
1	–	**8425.983** *8427.483*	**7713.163** *7714.711*	**7009.872** *7011.471*	**6316.044** *6317.674*	–	–	**4290.221** *4292.02*
2	–	**8968.00** *8969.47*	**8255.20** *8256.69*	**7551.88** *7553.44*	–	**6173.59**	**5498.37**	–
3	–	**9499.31** *9500.73*	**8786.44**	–	–	**6704.87** *6706.23*	–	–

Note. The upper figures are the band origins (in cm^{-1}) and the lower ones represent the position of the bandheads (when observed).

reported by Field and co-workers in the $C'^1\Sigma^+$–$A'^1\Pi$ (*17*), $E^1\Sigma^-$–$A'^1\Pi$ (*18*), $F^1\Pi$–$A'^1\Pi$, and $B^1\Pi$–$A'^1\Pi$ (*19*) systems. However, for $v' = 1$ and 2 very few combination differences can be deduced from the previous work (*17–19*), and this comparison is not very conclusive. (We note also that the maximum J values that we observed for these levels are much larger than those obtained in the laser studies (*17–19*)). The $v' = 3$ vibrational level was observed for the first time in the present work. The main check on our assignments of the perturbed $A'^1\Pi$ $v' = 3$ levels was the simultaneous presence of the same v' level in at least three bands involving different vibrational levels of the ground state.

Good agreement was generally observed between our spectra and the predictions of Field (*10*) for the $A'^1\Pi$–$X^1\Sigma^+$ transition, based on the deperturbation analysis of the $A^1\Sigma^+$–$X^1\Sigma^+$ system (*7, 9*). The positions of the bands that we identified agree well (within the uncertainty stated by the author) with the positions predicted in Table X of Ref. (*10*). This is also true for the relative intensities predicted by Field (*10*) from the Franck–Condon factors (note that the figures displayed in Table X of Ref. (*10*) are relative intensities of the v'–v'' bands sharing a common v' upper vibrational level).

The behavior of the Franck–Condon factors explains the absence of some vibrational bands in our spectrum, e.g., the 1–5, 1–6, 2–4, 3–3, and 3–4 bands (see Table 1). These bands are not present among Field's predictions (*10*) for the strongest bands of the $A'^1\Pi$–$X^1\Sigma^+$ system. Note, however, that we identified other bands (e.g., the 0–1, 0–2, 1–7, 2–6, etc., bands, see Table 1) which are not displayed in Table X of Ref. (*10*). Despite our efforts, no v'–0 vibrational bands could be identified in our spectra.

2. Data Analysis

The data analyses reported herein were performed using the program DSParFit (*38*) which was developed for fitting diatomic spectroscopic data involving one or more isotopomers and one or more electronic states to a variety of parameterized level energy expressions (see Refs. (*36, 37, 39–47*) for illustrative applications of this program). This program weights each experimental datum by the inverse square of its estimated uncertainty, and the quality of the fit is indicated by the dimensionless standard error $\bar{\sigma}_f$, which has a value of about 1.0 when, on average, the deviations from the model match the experimental uncertainties. All of our new data were assigned uncertainties of 0.005 cm^{-1}. The eight millimeter-wave (*21, 22*) and 41 infrared (*23, 24*) data available in the literature were combined with our 3009 A'–X lines in order to provide the best possible overall description of the $v'' = 0$–7 vibrational levels of the $X^1\Sigma^+$ ground state of CaO. The millimeter-wave and infrared data were weighted using the respective estimated uncertainties reported in Refs. (*21–24*).

While the ground state of CaO is known to be well-behaved, vibrational levels $v' \geq 2$ of the $A'^1\Pi$ state were found to be heavily perturbed. The present analysis therefore utilizes DSParFit's ability to use different types of representations for different electronic states and/or for different subsets of the data (*38*). In particular, the preliminary stage of the present analysis involved fits to the expression

$$\nu(v', J', p'; v'', J'') = T(v', J', p') - \sum_{m=0}^{l_{\max}(m)} \sum_{l} Y_{l,m}(v + 1/2)^l [J(J+1)]^m, \quad [1]$$

in which the levels of the ground state were represented by a conventional Dunham expansion (*48*), while the term value $T(v', J', p')$ (where p' is the parity label for the rotational levels of the $A'^1\Pi$ state, with values e or f) of each observed level of the A' state was treated as an independent parameter in the fit. This term-value treatment of the upper A-state levels is a type of procedure suggested by Åslund (*49*). However, it may also be thought of as a sorting of the electronic vibrational band data into groups of lines associated with distinct upper state levels, followed by an analysis which treats those groups as fluorescence series; this is what DSparFit does. For the present data set this involves "fluorescence series" associated with some 560 levels of A'-state CaO. This type of approach seems desirable, as our data set involves perturbed upper state vibrational levels (especially $v' = 2$ and 3), and this allows us to "disconnect" the unperturbed X-state levels from the perturbed A'-state ones without first converting the electronic data into a set of combination differences. The estimated experimental line position uncertainties of 0.005 cm^{-1} can then be used directly to weight the data.

The presence of perturbations in a given electronic state can be discerned in a variety of ways, the first and most common one being difficulty in the assignment of the spectral lines. Another signature is unusual behavior of the splitting or average of the term values corresponding to e and f parity in a given rotational series. Using the A'-state term values determined in our preliminary analysis, Fig. 3 shows the dependence on $J(J+1)$ of the quantities

$$[T_e(v', J') - T_f(v', J')]/[J'(J'+1)] \quad [2]$$

for A'-state vibrational levels $v' = 0$–3. For a $^1\Pi$ electronic state exhibiting Λ-doubling, this quantity is normally equal to (*50*) $q_B(v') + q_D(v')[J'(J'+1)]$, in which case the plots in Fig. 3 would be expected to be straight lines with slopes $q_D(v')$. This "normal" behavior can be seen in Fig. 3 for the $v' = 0$ and 1 vibrational levels, but the plots for $v' = 2$ and 3 deviate sharply from linearity, indicating the significant perturbation of those levels.

Another illustration of the perturbation of the upper v' levels of the A' state is provided by Fig. 4, which shows the depen-

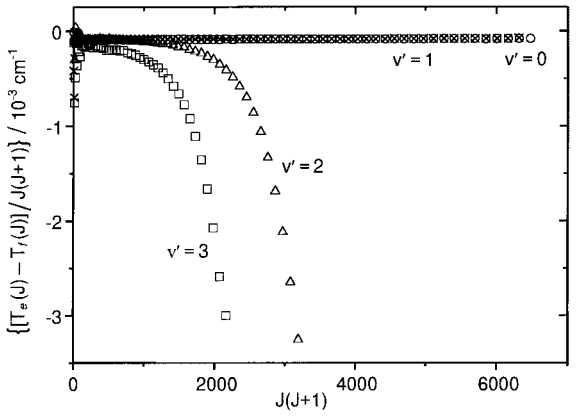

FIG. 3. The evolution (as a function of $J(J+1)$) of the difference between the term values corresponding to the *e* and *f* parities of the observed *J* rotational levels of the $v' = 0$, 1, 2, and 3 vibrational levels of the $A'\,{}^1\Pi$ upper state, divided by $J(J+1)$ (see text).

dence on $J'(J'+1)$ of the arithmetic mean of the *e*/*f* term values, divided by $J'(J'+1)$:

$$[T_e(v', J') + T_f(v', J') - 2T(v', 0)]/2[J'(J'+1)]. \quad [3]$$

For unperturbed levels this quantity is expected to be approximately (*50*) $B_{v'} - D_{v'}[J'(J'+1)]$, which would yield a straight line of slope $-D_{v'}$ and intercept $B_{v'}$ for these plots. Once again, normal behavior is observed for the $v' = 0$ and 1 levels, while the anomalous curves seen for $v' = 2$ and 3 indicate that those levels are affected by strong perturbations. These curves could also indicate an asymmetry in the perturbation of the *e* and *f* levels of the $A'\,{}^1\Pi$ $v' = 2$ and 3 levels.

Figures 3 and 4 show that although they may also be somewhat perturbed, A'-state levels $v' = 0$ and 1 may be effectively treated as "regular" Λ-doubled levels. In our final analysis of the data for this state, their term values were therefore represented by band constants

$$\begin{aligned} T(v', J', p') &= T_{v'} + \sum_{m=1} K_m(0)[J'(J'+1)]^m \\ &\quad \pm \tfrac{1}{2} \sum_{m=1} q_m(v')[J(J+1)]^m \\ &= T_{v'} + [B_{v'} \pm \tfrac{1}{2} q_B(v')][J'(J'+1)] \\ &\quad -[D_{v'} \mp \tfrac{1}{2} q_D(v')][J'(J'+1)]^2 + \cdots, \end{aligned} \quad [4]$$

where the upper and lower of ± and ∓ are for *e* and *f* levels, respectively, $q_1(v') \equiv q_B(v')$, $q_2(v') \equiv q_D(v')$, and we have followed the usual convention that D_v is the only band constant preceded by a negative sign. As a result, in this final fit to Eq. [1], *X*-state term values were again represented by Dunham expansions, the $v' = 0$ and 1 A'-state term values by Eq. [4], and the $v' = 2$ and 3 A'-state term values $T(v', J', p')$ were treated as independent parameters. After some experimentation it was found that an optimum fit was obtained when the Dunham expansions for the ground state included $m = 0$–2 and vibrational expansions of order $l_{\max}(m) = 4$, 3, and 2 for $m = 0$, 1, and 2, respectively. However, the band-constant treatment of A'-state levels $v' = 0$ and 1 also required $m = 3$ ($H_{v'}$) coefficients. Since they would not contribute to our knowledge of the ground state and the resulting A'-state term values would have no statistical significance, "fluorescence series" consisting of only a single transition were omitted from the present analysis. However, those 40 omitted lines are still available for use in a deperturbation analysis of the A' state.

In view of the apparently smooth (albeit very sharply curved) functional behavior of the plots for $v' = 2$ and 3 seen in Figs. 3 and 4, we also tried performing fits in which those two A'-state vibrational levels were represented by the band constant expression of Eq. [4]. For $v' = 2$ data a good fit could be obtained if the rotational sum in Eq. [4] was extended to $m_{\max} = 5$ (M_v), but for $v' = 3$ data even extending this series to $m = 7$ did not suffice to give a good fit. However, since excellent fits to the data for $v' = 0$ and 1 only required $m_{\max} = 2$, this approach seemed inappropriate, and our final fit represented all $v' = 2$ and 3 vibration–rotation levels by individual term values.

Our final fit therefore involved 11 Dunham parameters for the *X* state, eight band constants, and four Λ-doubling constants for A'-state levels $v' = 0$ and 1, and 185 term values for the heavily perturbed $v' = 2$ and 3 levels of the A' state. The resulting parameters and their 95% confidence limit uncertainties are presented in Tables 2 and 3; these results were obtained using the "sequential rounding and refitting" procedure of the DSParFit program, which yields a final parameter set involving a minimum number of significant digits with no significant loss of accuracy in the predictions they provide (*40*). The dimensionless standard error of the fit was $\bar{\sigma}_f = 0.93$. The results of the fit (including a list of [calc. − obs.] values) and a complete listing of the experimental input data are available electroni-

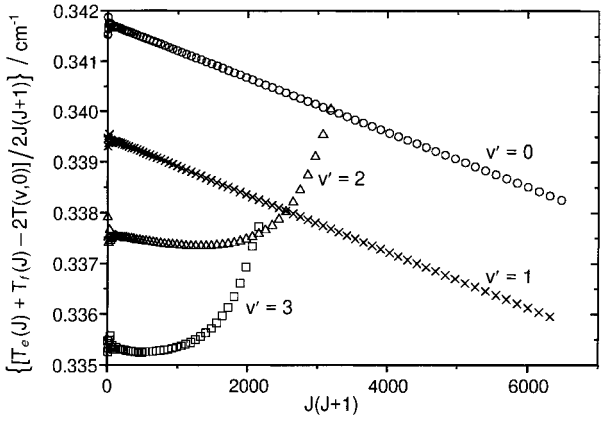

FIG. 4. The evolution (as a function of $J(J+1)$) of the arithmetic mean of the *e*/*f* term values divided by $J(J+1)$.

TABLE 2
Parameters (in cm^{-1}) for the $A'^1\Pi$–$X^1\Sigma^+$ System of $^{40}Ca^{16}O$

	$m=0$	$m=1$	$m=2$	$m=3$
$X\ ^1\Sigma^+$ State Dunham Constants				
$Y_{0,m}$	–	0.44443872 (18)	$-6.5418\,(48)\times10^{-7}$	
$Y_{1,m}$	732.01377 (140)	$-3.27456\,(36)\times10^{-3}$	$-8.25\,(16)\times10^{-9}$	
$Y_{2,m}$	−4.81268 (74)	$-2.058\,(18)\times10^{-5}$	$2.0\,(2)\times10^{-10}$	
$Y_{3,m}$	0.0020 (2)	$9.9\,(2)\times10^{-7}$		
$Y_{4,m}$	0.000861 (10)			
$A'\ ^1\Pi$ State Band Constants				
$K_m(v=0)$	8608.4386 (9)	0.341743 (1)	$-5.403\,(7)\times10^{-7}$	$1.9\,(5)\times10^{-13}$
$K_m(v=1)$	9148.7173 (9)	0.339471 (1)	$-5.657\,(6)\times10^{-7}$	$14.1\,(5)\times10^{-13}$
$A'\ ^1\Pi$ State Lambda-Doubling Constants				
$q_m(v=0)$	–	$-9.28\,(7)\times10^{-5}$	$2.2\,(2)\times10^{-9}$	
$q_m(v=1)$	–	$-9.04\,(8)\times10^{-5}$	$2.1\,(2)\times10^{-9}$	

Note. Numbers in parentheses are the 95% confidence limit uncertainties in the last significant digits shown.

cally on request from the authors or from the Journal's www page.

IV. DISCUSSION

To date, the most accurate Dunham parameters for the $X^1\Sigma^+$ ground state of CaO were those derived by Blom *et al.* (*25*) from a fit of eight millimeter-wave pure rotation (in $v'=0$ and 1) lines (*21*, *22*) and 41 infrared rovibrational (involving $v''=$ 0 to 3) lines (*23*, *24*). Our $A'^1\Pi$–$X^1\Sigma^+$ electronic data extend the high-resolution knowledge of the ground state to vibrational levels up to $v''=7$ and also to higher J rotational levels (J'' up to ~90, compared to 54 in the infrared study (*24*)). By merging the electronic, millimeter-wave, and infrared data sets in our least-squares treatment, one can expect improved and extended Dunham constants, so a comparison of parameters derived from our fit (presented in Table 2) and those obtained in the previous millimeter-wave/infrared work (*25*) is necessary.

In Table V of Ref. (*25*) it is interesting to note that a very long (in m) expansion was presented for the $Y_{l,m}$ constants (with m as high as six). These higher-order expansion terms were in fact derived from implicit relationships among the Dunham parameters, and not determined by experiment. In our case, we need only empirical T_v, B_v, and D_v constants to describe each vibrational level of the ground state, so we decided to use only the Dunham m series corresponding to these parameters (i.e., Y_{i0}, Y_{i1}, and Y_{i2}). With this expansion, the experimental data (including the millimeter-wave and infrared data) are well represented within the limits of the experimental precision (rms deviation = 0.89). Note, however, that we needed longer (by one unit) vibrational expansions for T_v's, B_v's, and D_v's than did the previous work of Blom *et al.* (*25*) because our data extended to $v''=7$, instead of $v''=3$.

Our constants are in good agreement with those of Blom *et al.* (*25*), especially for the first ℓ's of the $Y_{\ell,m}$ expansions, and the calculated uncertainties are systematically smaller (see Table 2 of the present work and Table V of Ref. (*25*)). However, for higher ℓ values this agreement deteriorates, although the corresponding values remain of the same order of magnitude. This occurs because of the different orders used in the Dunham expansions and the different v'' ranges.

High v'' vibrational levels of the $X^1\Sigma^+$ ground state of CaO were also observed by Brewer and Hauge (*9*), and effective rotational constants were derived for $v''\le 8$. However, the limited resolution of those photographic measurements restricted the precision of the constants. In his deperturbation study, Field (*10*) used the data of Hultin and Lagerqvist (*7*) and Brewer and Hauge (*9*) in a weighted least-squares fit to get improved B_e and α_e constants for the ground state, but they are still two orders of magnitude less precise than those derived in the present work.

A great advantage of the FTS recording of the $A'^1\Pi$–$X^1\Sigma^+$ transition is the fact that it permits a direct high-resolution linkage between the orange and green bands of CaO (involving $A'^1\Pi$, $a^3\Pi$, and $b^3\Sigma^+$ as lower states) and the infrared bands (involving the $X^1\Sigma^+$ ground state as the lower state). Indeed, up to now the linkage between these systems has been provided indirectly by the $B^1\Pi$–$X^1\Sigma^+$ blue system studied in the early 1950s by Lagerqvist (*8*) using photographic plates. The intrinsically precise laser measurements (*20*) are limited by the lack of a direct connection to the ground state. A new set of absolute term values for the excited states of CaO has now been derived from our study.

Although the main focus of this $A'^1\Pi$–$X^1\Sigma^+$ study has been on the $X^1\Sigma^+$ ground state, some very interesting features were revealed in the $A'^1\Pi$ perturbations. First, the present study permits the different vibrational levels to be positioned accurately with respect to each other. This has not been possible until now, as no $\Delta v\neq 0$ bands were observed in transitions

TABLE 3

Term Values (in cm^{-1}) for the $v = 2$ and 3 Vibrational Levels of the $A'^1\Pi$ State of $^{40}Ca^{16}O$ Expressed Relative to the X State ($v'' = 0$, $J'' = 0$) Level

J	$T_f(v=2)$	$T_e(v=2)$	$T_f(v=3)$	$T_e(v=3)$
3	9694.4400 (46)	9694.4501 (53)		
4	9697.1461 (46)	9697.1400 (41)		
5	9700.5240 (46)	9700.5251 (37)		
6	9704.5699 (46)	9704.5652 (37)	10235.8067 (64)	10235.7916 (46)
7	9709.2972 (46)	9709.2910 (35)	10240.4876 (53)	10240.4816 (46)
8	9714.6980 (41)	9714.6931 (37)	10245.8604 (53)	10245.8454 (53)
9	9720.7767 (41)	9720.7667 (35)	10251.8952 (53)	10251.8713 (46)
10	9727.5272 (41)	9727.5210 (35)	10258.5965 (53)	10258.5800 (46)
11	9734.9540 (41)	9734.9421 (35)	10265.9808 (53)	10265.9606 (46)
12	9743.0551 (41)	9743.0378 (35)	10274.0256 (53)	10274.0002 (53)
13	9751.8300 (41)	9751.8123 (33)	10282.7466 (53)	10282.7199 (46)
14	9761.2811 (41)	9761.2626 (33)	10292.1322 (53)	10292.1064 (46)
15	9771.4053 (41)	9771.3834 (33)	10302.1933 (53)	10302.1606 (46)
16	9782.2089 (46)	9782.1833 (33)	10312.9265 (53)	10312.8797 (46)
17	9793.6807 (41)	9793.6542 (33)	10324.3236 (53)	10324.2774 (41)
18	9805.8285 (41)	9805.7989 (33)	10336.3965 (53)	10336.3396 (46)
19	9818.6484 (41)	9818.6186 (35)	10349.1375 (53)	10349.0756 (46)
20	9832.1478 (41)	9832.1113 (33)	10362.5518 (53)	10362.4784 (46)
21	9846.3193 (41)	9846.2769 (31)	10376.6330 (53)	10376.5420 (46)
22	9861.1618 (41)	9861.1196 (33)	10391.3926 (53)	10391.2945 (46)
23	9876.6838 (41)	9876.6310 (31)	10406.8250 (53)	10406.7184 (41)
24	9892.8779 (41)	9892.8222 (35)	10422.9240 (53)	10422.8091 (41)
25	9909.7473 (41)	9909.6822 (31)	10439.6955 (53)	10439.5649 (41)
26	9927.2843 (41)	9927.2181 (38)	10457.1404 (53)	10457.0010 (41)
27	9945.5021 (41)	9945.4277 (31)	10475.2663 (53)	10475.0965 (41)
28	9964.3920 (41)	9964.3082 (31)	10494.0615 (53)	10493.8700 (41)
29	9983.9560 (41)	9983.8658 (35)	10513.5313 (53)	10513.3133 (41)
30	10004.1949 (41)	10004.0951 (31)	10533.6864 (53)	10533.4318 (46)
31	10025.1102 (41)	10024.9993 (33)	10554.5161 (53)	10554.2251 (41)
32	10046.6999 (46)	10046.5743 (35)	10576.0319 (53)	10575.6926 (41)
33	10068.9639 (41)	10068.8282 (35)	10598.2317 (53)	10597.8382 (41)
34	10091.9075 (42)	10091.7550 (35)	10621.1144 (53)	10620.6558 (46)
35	10115.5271 (42)	10115.3559 (35)	10644.7110 (53)	10644.1632 (42)
36	10139.8236 (42)	10139.6373 (36)	10669.0044 (53)	10668.3408 (46)
37	10164.8021 (42)	10164.5907 (38)	10694.0080 (53)	10693.1987 (42)
38	10190.4612 (42)	10190.2152 (36)	10719.7320 (54)	10718.7578 (42)
39	10216.7997 (42)	10216.5272 (39)	10746.2071 (54)	10745.0054 (42)
40	10243.8313 (43)	10243.5095 (39)	10773.4473 (54)	10771.9368 (43)
41	10271.5468 (48)	10271.1810 (40)	10801.4830 (54)	10799.5805 (43)
42	10299.9596 (43)	10299.5334 (40)	10830.3659 (55)	10827.9252 (43)
43	10329.0700 (44)	10328.5617 (44)	10860.1364 (55)	10856.9967 (44)
44	10358.8868 (45)	10358.2874 (44)	10890.8860 (55)	10886.7894 (44)
45	10389.4213 (45)	10388.6885 (45)	10922.6673 (56)	10917.3190 (49)
46	10420.6810 (46)	10419.7931 (46)		10948.6198 (50)
47	10452.6852 (47)	10451.5905 (46)		10980.6749 (57)
48	10485.4570 (58)	10484.0856 (52)		11013.5515 (58)
49	10519.0210 (59)	10517.3131 (53)		
50	10553.4321 (70)	10551.2382 (70)		
51		10585.9036 (71)		
52		10621.2988 (72)		
53		10657.4484 (73)		
54		10694.3694 (75)		
55		10732.0884 (76)		
56		10770.6263 (78)		

Note. Numbers in parentheses are the 95% confidence limit uncertainties in the last significant digits shown.

involving the $A'^1\Pi$ state as lower level (*17–19*), with the single exception of the $B^1\Pi$–$A'^1\Pi(1, 0)$ band (*19*), but in that case only the $v = 0$ vibrational level of the $A'^1\Pi$ state was observed. A low-resolution study (*12*) of the $A'^1\Pi$–$X^1\Sigma^+$ system gave access to high vibrational levels ($9 \le v' \le 21$) of the $A'^1\Pi$ state and provided the vibrational constants values $\omega'_e = 545.7(8)$ cm^{-1} and $\omega_e x'_e = 2.54(3)$ cm^{-1}. The fundamental vibrational spacing $\Delta G'_{1/2} = 540.6$ cm^{-1} obtained in that study is in surprisingly good agreement with the value $\Delta G'_{1/2} = 540.279(1)$ cm^{-1} implied by the results listed in Table 2 of the present work. Note also that relatively good agreement is obtained between the $A'^1\Pi$ $v' = 0$ term values and those derived by Norman *et al.* (*16*, Table 4), especially for low J levels (although a 0.05 cm^{-1} systematic deviation is observed, probably due to calibration problems). This agreement slowly deteriorates with increasing J to $\sim$0.2 cm^{-1} at $J = 69$. The constants derived from our analysis of the $A'^1\Pi$ $v = 0$ and 1 levels are in reasonable agreement with those published in various studies (*16–19*). The higher J's observed in the present work allowed us to determine the additional Λ-doubling parameter q_D, as well as an H_v constant for each "unperturbed" vibrational level (see Table 2). It is likely that these additional constants are affected by perturbations. Some evidence for this conclusion is provided by the very different magnitudes of the $H_{v'}$ constants determined for $v' = 0$ and 1.

In the previous sections, we referred to the $v' = 0$ and 1 vibrational levels of the $A'^1\Pi$ upper state as unperturbed (or "less perturbed") compared to the $A'^1\Pi$ $v = 2$ and 3 levels, which were said to be "perturbed." This view is based on the appearance of the spectrum, on the ease of making line assignments, and finally on the fit using a classical polynomial expansion. In fact a significant interaction between the vibrational levels of the $A'^1\Pi$ and $a^3\Pi$ states does take place. Baldwin *et al.* (*18*) treated this interaction for the $a^3\Pi$ ($v = 0$) $\sim$ $A'^1\Pi$ ($v = 0$) pair of levels in a deperturbation analysis. The relatively large separation between these two vibrational levels ($\sim$300 cm^{-1}) and nearly identical rotational constants (*18*) results in a rather "smooth" perturbation with the two sets of rotational levels remaining almost parallel and $\sim$300 cm^{-1} from each other for the same J value. This pattern should then repeat for each given v of the $a^3\Pi(v)$ $\sim$ $A'^1\Pi(v)$ pair of levels, because the vibrational constants of the $a^3\Pi$ and $A'^1\Pi$ electronic states are almost identical. This interaction does not result in any level crossings (i.e., no extra lines), and the energy levels will be well represented by a polynomial fit to effective constants (even if they are perturbed and not "mechanical" constants), as was the case for the $A'^1\Pi$ $v = 0$ and 1 vibrational levels in the present work (see Table 2 and Figs. 3 and 4). The $A'^1\Pi$ and $a^3\Pi$ states do not strongly interact with the $A^1\Sigma^+$ state until $v = 6$.

However, the $A'^1\Pi$ $v = 2$ and 3 levels are found to be much more massively perturbed than $v = 0$ and 1. This is surprising at first sight, but there is another electronic state in this region, namely $b^3\Sigma^+$, identified through the observation of the $B^1\Pi$–$b^3\Sigma_0^+(1, 1)$ band (*20*). Examining the $A'^1\Pi$ $v = 3$ term values listed in Table 3 and those for the $b^3\Sigma^+$ $v = 1$ and $a^3\Pi$ $v = 3$ displayed in Table I of Ref. (*20*), one sees that the $A'^1\Pi$ ($v = 3$, J) and $b^3\Sigma_0^+$ ($v = 1$, J) levels, separated by $\sim$114

cm^{-1} at $J = 14$, become closer as J increases ($\sim$86 cm^{-1} separation at $J = 25$), while the $A'^1\Pi$ ($v = 3$, J)–$a^3\Pi$ ($v = 3$, J) separation remains almost constant at $\sim$275 cm^{-1}. Consequently, only the $A'^1\Pi$ ($v = 3$) $\sim$ $b^3\Sigma^+$ ($v = 1$) interaction can explain the very peculiar behavior of the $A'^1\Pi$ ($v = 3$) level observed in Figs. 3 and 4. Because the estimated vibrational constant ($\omega_e \sim 580$ cm^{-1}) for the $b^3\Sigma^+$ state (*20*) is not very different from that of the $A'^1\Pi$ electronic level ($\omega_e \sim 545$ cm^{-1}), the corresponding $A'^1\Pi$ ($v = 2$) $\sim$ $b^3\Sigma^+$ ($v = 0$) interaction should also be responsible for the behavior of the $A'^1\Pi$ ($v = 2$) vibrational level. The difference in the vibrational constants of the $A'^1\Pi$ and $b^3\Sigma^+$ states ($\sim$35 cm^{-1}) results in a larger separation (approximately by this amount) between the levels of the $A'^1\Pi$ ($v = 2$) $\sim$ $b^3\Sigma^+$ ($v = 0$) pair, compared to those of the $A'^1\Pi$ ($v = 3$) $\sim$ $b^3\Sigma^+$ ($v = 1$) pair, and this fact explains the smaller perturbation of the $A'^1\Pi$ ($v = 2$) levels.

Note that only the $b^3\Sigma^+_{0^-}$ levels were observed in the previous study of Baldwin and Field (*20*), and the $A'^1\Pi$ state should experience a strong homogeneous spin–orbit interaction (*51*) with the $b^3\Sigma^+_1$ component, which must be near $b^3\Sigma^+_{0^-}$. The $A'^1\Pi$ state can interact directly with the $b^3\Sigma^+$ state through the microscopic form of the spin–orbit operator (*51*):

$$\hat{H}_{so} = \sum_i a_i \vec{l}_i \cdot \vec{s}_i = \sum_i a_i (\hat{l}_z \hat{s}_z + \tfrac{1}{2}(\hat{l}_+ \hat{s}_- + \hat{l}_- \hat{s}_+)).$$

The $A'^1\Pi$ state is represented by the (Ca)σ^1(O)$p\pi^{-1}$ configuration and $b^3\Sigma^+$ by the (Ca)σ^1(O)$p\sigma^{-1}$ configuration. The spin–orbit operator has a nonzero matrix element between $A'^1\Pi_1$ and $b^3\Sigma^+_1$,

$$H_{v^*v} = \langle v^*;\, b^3\Sigma^+_1 | \hat{H}_{so} | A'^1\Pi_1;\, v\rangle = \frac{1}{\sqrt{2}}\, a \langle v^* | v\rangle,$$

assuming that the (O)$p\sigma$ and (O)$p\pi$ orbitals can be represented as oxygen p orbitals. The $\langle v^*|v\rangle$ integral is a vibrational overlap whose square is a Franck–Condon factor. A value for the atomic spin–orbit parameter a can be estimated as -121 cm^{-1} from the value tabulated for O^- by Lefebvre-Brion and Field (*51*).

A complete deperturbation treatment needs to be carried out for the various electronic states present in the $\sim$1 eV $< E <$ $\sim$2 eV region of the energy level diagram. Once the analysis of the $A^1\Sigma^+$–$X^1\Sigma^+$ system (*30*) is completed, we intend to perform such an $a^3\Pi \sim A'^1\Pi \sim b^3\Sigma^+ \sim A^1\Sigma^+$ multistate deperturbation study.

V. CONCLUSION

We recorded the first high-resolution spectrum of the $A'^1\Pi$–$X^1\Sigma^+$ near-infrared system of CaO using a Fourier transform spectrometer. The CaO molecules were produced in a Broida-type oven by the exothermic reaction between Ca vapor and N_2O gas. The observation of this transition provides a direct high-resolution linkage between the orange–green bands of CaO (involving $A'^1\Pi$, $a^3\Pi$, and $b^3\Sigma^+$ as lower states) and the near-infrared systems (involving the $X^1\Sigma^+$ ground state as the lower state).

A total of 3009 rotational lines were assigned in 19 vibrational bands joining the $0 \le v' \le 3$ vibrational levels of the $A'^1\Pi$ upper state to the $X^1\Sigma^+$ $1 \le v'' \le 7$ ground state levels. This study extends the high-resolution knowledge of the vibrational levels of the ground state up to $v'' = 7$. An improved set of Dunham constants was derived for the $X^1\Sigma^+$ state from a least-squares fitting of our data, together with millimeter-wave and infrared data available in the literature.

The observed vibrational levels of the $A'^1\Pi$ upper state are found to be heavily perturbed, especially in the case of $v' = 2$ and 3. These perturbations are explained by a strong $\Delta v = 2$ interaction between close-lying $A'^1\Pi$ ($v \ge 2$) and $b^3\Sigma^+$ ($v - 2$) levels. Thus, while band constants could be effectively used for transitions involving A'-state levels $v' = 0$ and 1, a term value representation was necessary for $v' = 2$ and 3 in our least-squares treatment. We intend to use our $A'^1\Pi$ observations in a multistate deperturbation analysis of the $a^3\Pi \sim A'^1\Pi \sim b^3\Sigma^+ \sim A^1\Sigma^+$ complex of excited states.

ACKNOWLEDGMENTS

This work was supported by the National Sciences and Engineering Research Council of Canada (NSERC). Partial support was also provided by the Petroleum Research Fund of the American Chemical Society. The Centre d'Etudes et de Recherches Lasers et Applications is supported by the Ministère chargé de la Recherche, the Région Nord-Pas de Calais, and the Fonds Européen de Développement Economique des Régions. We thank R. Engleman for providing the Ca atomic line positions in advance of publication.

REFERENCES

1. P. C. Mahanti, *Phys. Rev.* **42,** 609–621 (1932).
2. P. H. Brodersen, *Z. Phys.* **79,** 613–625 (1932).
3. P. H. Brodersen, *Z. Physik* **104,** 135–156 (1937).
4. W. F. Meggers, *Bur. Stand. J. Res.* **10,** 669–684 (1933).
5. J.-M. Lejeune, *Bull. Soc. Roy. Sci. Liège* **14,** 318–321 (1945).
6. J.-M. Lejeune and B. Rosen, *Bull. Soc. Roy. Sci. Liège* **14,** 322 (1945).
7. M. Hultin and A. Lagerqvist, *Ark. Fys.* **2,** 471–507 (1950).
8. A. Lagerqvist, *Ark. Fys.* **8,** 83–95 (1954).
9. L. Brewer and R. Hauge, *J. Mol. Spectrosc.* **25,** 330–339 (1968).
10. R. W. Field, *J. Chem. Phys.* **60,** 2400–2413 (1974).
11. L. Brewer and J. L. Wang, *J. Chem. Phys.* **56,** 4305–4309 (1972).
12. R. W. Field, G. A. Capelle, and C. R. Jones, *J. Mol. Spectrosc.* **54,** 156–159 (1975); *J. Mol. Spectrosc.* **57,** 321 (1975).
13. G. A. Capelle, C. R. Jones, J. Zorskie, and H. P. Broida, *J. Chem. Phys.* **61,** 4777–4779 (1974).
14. R. F. Marks, H. S. Schweda, R. A. Gottscho, and R. W. Field, *J. Chem. Phys.* **76,** 4689–4691 (1982); *J. Chem. Phys.* **77,** 4795 (1982).
15. R. F. Marks, R. A. Gottscho, and R. W. Field, *Phys. Scr.* **25,** 312–328 (1982).
16. J. B. Norman, K. J. Cross, H. S. Schweda, M. Polak, and R. W. Field, *Mol. Phys.* **66,** 235–268 (1989).
17. D. P. Baldwin and R. W. Field, *J. Mol. Spectrosc.* **133,** 90–95 (1989).

18. D. P. Baldwin, J. B. Norman, R. A. Soltz, A. Sur, and R. W. Field, *J. Mol. Spectrosc.* **139,** 39–67 (1990).
19. D. P. Baldwin and R. W. Field, *J. Mol. Spectrosc.* **139,** 68–76 (1990).
20. D. P. Baldwin and R. W. Field, *J. Mol. Spectrosc.* **139,** 77–83 (1990).
21. R. A. Creswell, W. H. Hocking, and E. F. Pearson, *Chem. Phys. Lett.* **48,** 369–371 (1977).
22. W. H. Hocking, E. F. Pearson, R. A. Creswell, and G. Winnewisser, *J. Chem. Phys.* **68,** 1128–1134 (1978).
23. C. E. Blom and H. G. Hedderich, *Chem. Phys. Lett.* **145,** 143–145 (1988).
24. H. G. Hedderich and C. E. Blom, *J. Chem. Phys.* **90,** 4660–4663 (1989).
25. C. E. Blom, H. G. Hedderich, F. J. Lovas, R. D. Suenram, and A. G. Maki, *J. Mol. Spectrosc.* **152,** 109–118 (1992).
26. W. B. England, *Chem. Phys.* **53,** 1–21 (1980).
27. K. D. Carlson, K. Kaiser, C. Moser, and A. C. Wahl, *J. Chem. Phys.* **52,** 4678–4691 (1970).
28. C. W. Bauschlicher, Jr. and D. R. Yarkony, *J. Chem. Phys.* **68,** 3990–3997 (1978).
29. R. N. Diffenderfer and D. R. Yarkony, *J. Chem. Phys.* **77,** 5573–5580 (1982).
30. C. Focsa, B. Pinchemel, and P. F. Bernath, unpublished manuscript.
31. J. B. West, R. S. Bradford, Jr., J. D. Eversole, and C. R. Jones, *Rev. Sci. Instrum.* **46,** 164–168 (1975).
32. P. F. Bernath, *Adv. Photochem.* **23,** 1–61 (1997).
33. B. Edlén, *Metrologia* **2,** 71–80 (1966).
34. K. P. Birch and M. J. Downs, *Metrologia* **30,** 155–162 (1993).
35. R. Engleman, private communication.
36. H. Li, C. Focsa, B. Pinchemel, R. J. LeRoy, and P. F. Bernath, *J. Chem. Phys.* **113,** 3026–3033 (2000).
37. H. Li, R. Skelton, C. Focsa, B. Pinchemel, and P. F. Bernath, submitted for publication.
38. R. J. Le Roy, DSParFit 1.0. A Computer Program for Fitting Multi-Isotopomer Diatomic Molecule Spectra, University of Waterloo Chemical Physics Research Report CP-646, 2000. [The source code and manual for this program may be obtained from the www site http://theochem.uwaterloo.ca/~leroy.]
39. R. J. Le Roy, *J. Mol. Spectrosc.* **194,** 189–196 (1999).
40. R. J. Le Roy, *J. Mol. Spectrosc.* **191,** 223–231 (1998).
41. E. G. Lee, J. Y. Seto, T. Hirao, P. F. Bernath, and R. J. Le Roy, *J. Mol. Spectrosc.* **194,** 197–202 (1999).
42. T. Parekunnel, T. Hirao, R. J. Le Roy, and P. F. Bernath, *J. Mol. Spectrosc.* **195,** 185–191 (1999).
43. J. Y. Seto, Z. Morbi, F. Charron, S. K. Lee, P. F. Bernath, and R. J. Le Roy, *J. Chem. Phys.* **110,** 11756–11767 (1999).
44. S. A. Beaton and M. C. L. Gerry, *J. Chem. Phys.* **110,** 10715–10724 (1999).
45. Y. Liu, J. Li, D. Chen, L. Li, K. M. Jones, B. Ji, and R. J. Le Roy, *J. Chem. Phys.* **111,** 3494–3497 (1999).
46. C. Focsa, H. Li, and P. F. Bernath, *J. Mol. Spectrosc.* **200,** 104–119 (2000).
47. J. Y. Seto, R. J. Le Roy, J. Vergès, and C. Amiot, *J. Chem. Phys.*, in press.
48. J. L. Dunham, *Phys. Rev.* **41,** 721–731 (1932).
49. N. Åslund, *J. Mol. Spectrosc.* **50,** 424–434 (1974).
50. P. F. Bernath, "Spectra of Atoms and Molecules," Oxford University Press, New York, 1995.
51. H. Lefebvre-Brion and R. W. Field, "Perturbations in the Spectra of Diatomic Molecules," Academic Press, New York, 1986.